Uniaxial-stress effects on the electronic properties of carbon nanotubes

R. Heyd and A. Charlier
Laboratoire de Physique du Solide, 1 boulevard Arago, 57078 Metz Cedex 03, France

E. McRae
Laboratoire de Chimie du Solide Minéral, URA 158 CNRS, Boîte Postale 239, 54506 Vandoeuvre les Nancy, France

(Received 6 September 1996)

Using a semiempirical tight-binding approach modified through introduction of a deformation potential, we have calculated the effects of uniaxial stress on the electronic density of states of carbon tubules. For zigzag tubules $(n,0)$ the gap varies linearly with stress and independently of diameter: $|dE_{\mathrm{gap}}/d\sigma| = 10.7$ meV/GPa for $|\sigma| < 10$ GPa, and a semiconductor to metal transition is predicted. The behavior is strongly dependent on whether $n = 3q, 3q-1, 3q+1$. The armchair tubules remain metallic under all conditions studied. [S0163-1829(97)02411-9]

I. INTRODUCTION

Since graphitic tubules with radii of a few nanometers (carbon nanotubes) were discovered by Iijima[1] under roughly the same conditions as those used to produce the fullerenes, quite intense activity has been undertaken in both experimental and theoretical fields. Early theoretical studies[2–5] showed that these nanotubes exhibit some unexpected and very interesting electronic properties; indeed they may be metallic or narrow- or moderate-gap semiconductors depending simply on geometric characteristics, e.g., diameter and chirality. In some respects, this is certainly an unexpected feature since other than the effects linked to bending the graphene [two-dimensional (2D) graphite] sheets to form the tubes (significant in small-diameter tubes and not taken into account in the early theoretical works), the trigonal configuration of the component carbon atoms is the same in all cases. Such differences in electronic properties depend on whether the allowed k-space states pass through the K points of the 2D graphene Brillouin zone. Later studies of band structure went beyond the ''graphene model'' and took into account the effects of curvature.[6]

We first present the π electron density of states (DOS) of two particular, high-symmetry types of carbon nanotubes, designated zigzag and armchair tubules. We have used the Green's-function method within the framework of a simple, tight-binding scheme based on a 1D tubule model. We have computed an analytic expression of the DOS $\rho(E)$ and discuss the main features according to the type of tubule. Next, we particularly treat the effects of compressive and tensile, uniaxial stress on the DOS and the band gaps. This seems of interest since such effects of stress on the electronic properties of carbon tubules have received little attention (to date) in spite of references to the predicted interesting mechanical properties.[7–10]

II. TUBULE MODELS

Using the notation of Refs. 6 and 11, a tubule is defined in terms of the two direct lattice vectors of a 2D graphite sheet $\mathbf{a}_1$ and $\mathbf{a}_2$ and a pair of integers (n,m) such that $\mathbf{C} = n\mathbf{a}_1 + m\mathbf{a}_2$, $\mathbf{C}$ being the chiral vector. For the zigzag tubule $m = 0$ and for the armchair $n = m$. The widely used model of a single-walled tubule consists of rolling up a semi-infinite sheet of graphene into a cylindrical tube of constant radius. Thus sp^2 hybridization of the 2D graphene honeycomb lattice, in addition to the Born–von Kármán periodic boundary conditions on the circumference $\mathbf{k}\cdot\mathbf{C} = 2\pi l$ (where l is an integer), plays a key role in the electronic properties of nanotubes. The Born–von Kármán condition cuts the hexagonal Brillouin zone of the graphene into L allowed parallel k lines separated by a distance $\Delta k = 2\pi/|\mathbf{C}|$. The positions of these lines in the Brillouin zone then define the electronic structure of the tube. Such a representation is a 2D tubule model.

Furthermore, a translation vector $\mathbf{T}$ can be defined, perpendicular to $\mathbf{C}$. The translation $\mathbf{T}$ and the rectangle defined by $\mathbf{R}$ and $\mathbf{T}$ completely define the tubule.[11] Such a 1D representation lends itself to an easier calculation of the DOS than does a 2D model using the Green's-function technique, as shown below.

As mentioned above, the graphene model[6] does not take into account the effect of curvature and predicts that the zigzag tubules for which n is a multiple of 3 are metallic. In fact, the curvature of small diameter tubes transforms the predicted metallic behavior into that of a small-gap semiconductor due to σ-π hybridization.[3,4,6] In the present case, to introduce the effects of curvature on the (1D) electronic properties, we use a simple deformation potential[12] as a perturbation in a tight-binding model[13] near the Fermi level.

III. DENSITY-OF-STATES CALCULATIONS

The Green's-function technique we have used in this work is formulated within the framework of a tight-binding Hamiltonian, which can be expressed by

$$\hat{H} = \sum_i |i\rangle \varepsilon_i \langle i| + \sum_{i,j} |i\rangle \alpha_{i,j} \langle j|. \tag{3.1}$$

If we neglect the effect of curvature, the values of the $\alpha_{i,j}$ intersite parameters are the same as those used by Charlier et al.[13] The site energies ε_i associated with the two different

sites A and B of a (2D) graphite sheet have the same values in the graphene model. Thus these energies are chosen as a reference and set equal to zero. $\{|i\rangle\}$ is a set of atomic or Wannier-type wave functions localized on site i. The Bloch monoelectronic wave functions of the tubules are given by

$$|\vec{k}\rangle = \frac{1}{\sqrt{N}} \sum_j e^{i\vec{k}\cdot\vec{R}_j} |j\rangle. \tag{3.2}$$

Since the σ and the π energy bands very weakly overlap in the case of graphene, we consider here the π DOS only. The electronic properties are obtained[14] from the projection on the preceding set of Bloch wave functions of the inverse operator associated with

$$\hat{g} = [\hat{I}z - \hat{H}]. \tag{3.3}$$

The partial density of π electronic states $\rho^{(m)}(E)$, which is associated with the mth allowed k line in the Brillouin zone of graphene, is deduced from the following analytic extension of the Green's function of the tubules:

$$G^{(m)\pm}(E \pm i\varepsilon) = \frac{\Omega}{2\pi N} \times \lim_{\varepsilon \to 0^+} \int_{(m)\text{line}} \frac{E \pm i\varepsilon}{(E \pm i\varepsilon)^2 - \left| \sum_B e^{i\vec{k}\cdot(\vec{R}_B - \vec{R}_A)} \alpha_{AB} \right|^2} dk, \tag{3.4}$$

where the integral is taken over the mth line by the expression

$$\rho^{(m)}(E) = \mp \frac{1}{\pi} \mathrm{Im}[G^{(m)\pm}(E \pm i\varepsilon)], \tag{3.5}$$

where Ω is the volume of the (1D) unit cell of the tubule and Im is the imaginary part. The total DOS is then given by the summation on the allowed k lines

$$\rho(E) = \sum_m \rho^{(m)}(E). \tag{3.6}$$

Using this technique,[14,15] we then computed an analytic expression of ρ(E) for $0 \leqslant E \leqslant 10$ eV in the cases of both types of nanotubes studied here. As noted in other calculations,[16] the curves obtained (Fig. 1) are characteristic of quasi-1D behavior. Indeed, we observe the formation of discrete energy levels E_m corresponding to DOS discontinuities (δ-like variations). Furthermore, integrating Eq. (3.4) by the residues theorem, we obtain analytical expressions of the DOS $\rho(E)$, which can be expressed in the form

$$\rho(E) = \sum_m \frac{|E|}{\sqrt{E^2 - E_m^2}\sqrt{E_m'^2 - E^2}}, \tag{3.7}$$

where E_m and E_m' are discrete energy values. This expression of $\rho(E)$ is different from that obtained for a confined 1D electron gas

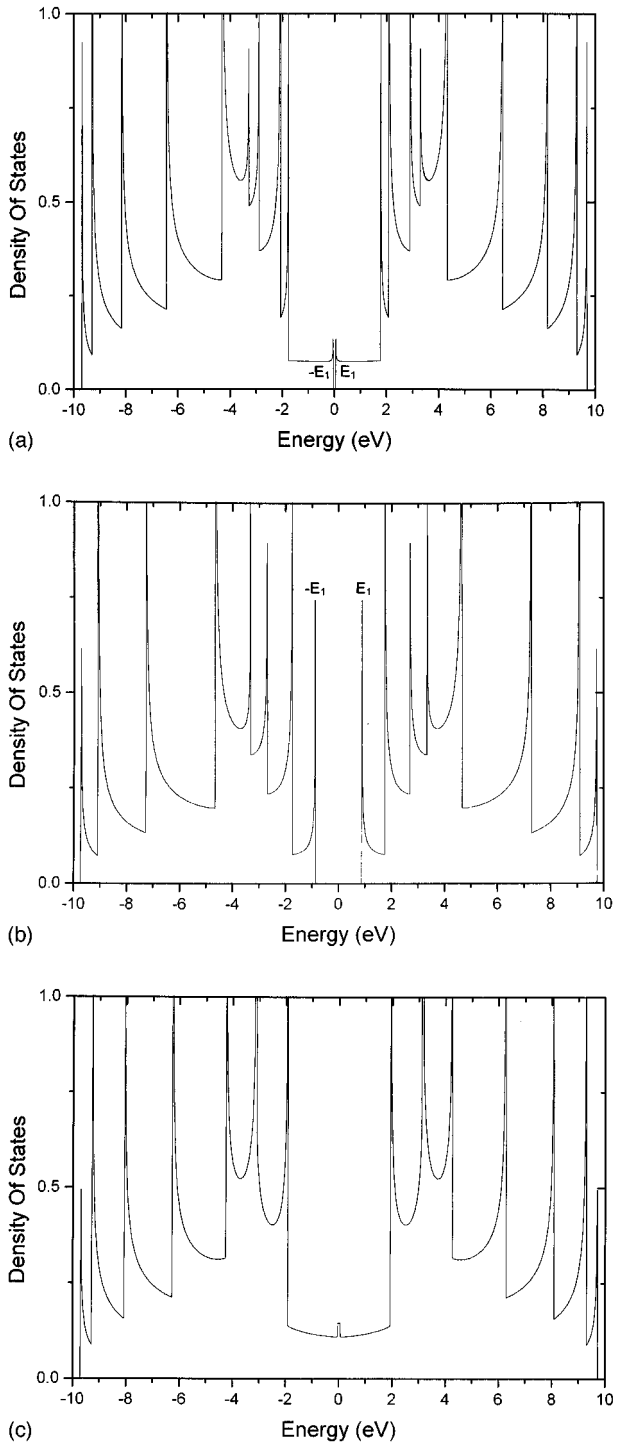

FIG. 1. Calculated DOS $\rho(E)$ for (a) and (b) zigzag and (c) armchair tubules. The parameters (n,m) are (9,0), (7,0), and (5,5), respectively.

$$\rho_{1D}(E) = \sum_m \alpha_m / \sqrt{E - E_m}. \tag{3.8}$$

Experimental evidence of such 1D confinement has been put forth through scanning tunneling spectroscopy[17] (STS). In these studies, conductance versus voltage curves (dI/dV) showed peaks that these authors associated with $1/\sqrt{E - E_0}$ discontinuities. Perhaps a more detailed line-shape

analysis of the STS data would allow distinguishing between Eqs. (3.7) and (3.8). In Figs. 1(a) and 1(b), the quantity $2E_1$ is the gap. Figure 1(a) shows that the deformation potential representing the effects of the curvature [α_{ij} in expression (3.1)] has indeed opened a small gap removing the strictly metallic character, initially predicted. Figure 1(c) illustrates the metallic behavior of the armchair tubules.

IV. EFFECTS OF UNIAXIAL STRESS

We now examine the effects of a uniaxial, homogeneous deformation of the tubules along their axes. We have computed the π-electron band structure and DOS, under both uniaxial traction ($\sigma>0$) and compression ($\sigma<0$) using a semiempirical tight-binding approach,[18] adapted to take into account the modifications of both direct and reciprocal lattice structures and two-center integrals with stress.

We have determined the new positions of the carbon atoms in a tubule submitted to a uniaxial stress σ, in the framework of elasticity theory assuming small strains using the relationship

$$\mathbf{R}_{i'}=(\underline{1}+\underline{\varepsilon})\mathbf{R}_i\,. \tag{4.1}$$

$\mathbf{R}_i$ and $\mathbf{R}_{i'}$ are the position vectors before and after stress of atom i. $\underline{1}$ is the unit matrix and $\underline{\varepsilon}$ is the reduced deformation tensor in the graphene plane.[19] In the case of uniaxial deformation of armchair and zigzag tubules $\underline{\varepsilon}$ takes the forms

$$\underline{\varepsilon}_{\text{armchair}}=\begin{pmatrix} S_{12}\sigma & 0 & 0\\ 0 & S_{11}\sigma & 0\\ 0 & 0 & 0\end{pmatrix},$$

$$\underline{\varepsilon}_{\text{zigzag}}=\begin{pmatrix} S_{11}\sigma & 0 & 0\\ 0 & S_{12}\sigma & 0\\ 0 & 0 & 0\end{pmatrix}. \tag{4.2}$$

We have used the graphite values[20] $S_{11}=0.98\times10^{-12}$ Pa^{-1} and $S_{12}=-0.16\times10^{-12}$ Pa^{-1}.

Using Eq. (4.1), the vectors of the deformed tubule unit cell are constructed. The 1D unit cell remains rectangular as shown in Fig. 2. Since the deformation also modifies the different carbon-carbon lengths it is necessary to recalculate the transfer integrals between the different atoms. To do so we have used Harrison's formula[18,21–23]

$$t_{\alpha\beta}=t^{(0)}_{\alpha\beta}\left(\frac{d_0}{d}\right)^{n_{\alpha\beta}}. \tag{4.3}$$

d_0 and d are the bond lengths before and after deformation. Since no experimental values of $n_{\alpha\beta}$ are available for tubules, we have used $n_{\alpha\beta}=2$ as done by Harrison himself, for all types of orbitals α,β. In our approach, we take into account only π orbitals; therefore, we no longer need α and β indices. In the case of elongated graphene, the carbon-carbon bonds are no longer equivalent and we will use the following notation: A_0 is taken as a reference atom and its three nearest neighbors are designated B_1, B_2, and B_3. If the A_0B_3 segment is parallel to the $(n,0)$ tubule's axis and

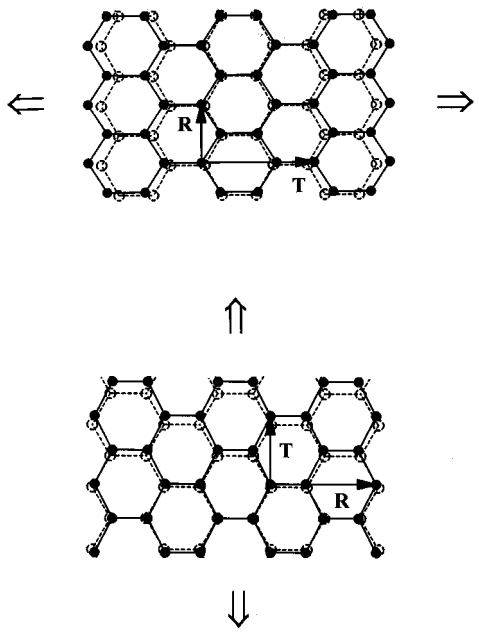

FIG. 2. Schematic representation of the effect of uniaxial tensile stress on a (1D) rectangular unit cell. From top to bottom, deformation along the $(n,0)$ zigzag axis and the (n,n) armchair axis. Dashed lines and circles represent the undeformed honeycomb lattice.

A_0B_1 and A_0B_2 are symetrically placed with respect to the same axis, then we define the transfer integrals $t_\pi^{A_0B_3}=t_3$ and $t_\pi^{A_0B_1}=t_\pi^{A_0B_2}=t_{12.}$

We find that the discrete DOS energy levels and the gaps are very deformation sensitive. For uniaxial strain, $\rho(E)$ still varies qualitatively as in Fig. 1 and is analytically expressed in the case of $(n,0)$ tubule by

$$\rho(E,\sigma)=\frac{1}{2\pi\sqrt{3}}\frac{(1+S_{12}\sigma)}{(1+S_{11}\sigma)}\sum_{(m)}\frac{|E|\,\theta(|E|,E_m^-)\,\theta_{\text{inv}}(|E|,E_m^+)}{\sqrt{E^2-(E_m^-)^2}\sqrt{(E_m^+)^2-E^2}}, \tag{4.4}$$

where the discrete energy levels E_m, displaced by the deformation, are given by

$$E_m^{\pm}(\sigma)=t_3\left|\left[1\pm2\left(\frac{t_{12}+V_{12}}{t_3}\right)\cos\frac{m\pi}{N_{\text{C}}}\right]\right|. \tag{4.5}$$

$\theta(|E|,E_m^-)$ and $\theta_{\text{inv}}(|E|,E_m^+)$ are, respectively, the Heaviside and the inverse Heaviside function defined by $\theta(|E|,E_m^-)=1$ if $|E|>E_m^-$ and 0 elsewhere and $\theta_{\text{inv}}(|E|,E_m^+)=1$ if $|E|<E_m^+$ and 0 elsewhere.

Using the same ij notation as for the t_{ij} transfer integrals, the V_{ij} are parameters that take into account the effect of curvature of the graphene under conformal transformation. N_{C} is the number of carbon atoms on the $(n,0)$ tubule's circumference.

We obtain similar expressions for $\rho(E)$ and E_m in the case of armchair (n,n) tubules. These results are of less importance since these tubules remain metallic under all strains studied here.

Let us examine the $(n,0)$ zigzag tubules. It is always possible to define the zigzag tubules in one of the following

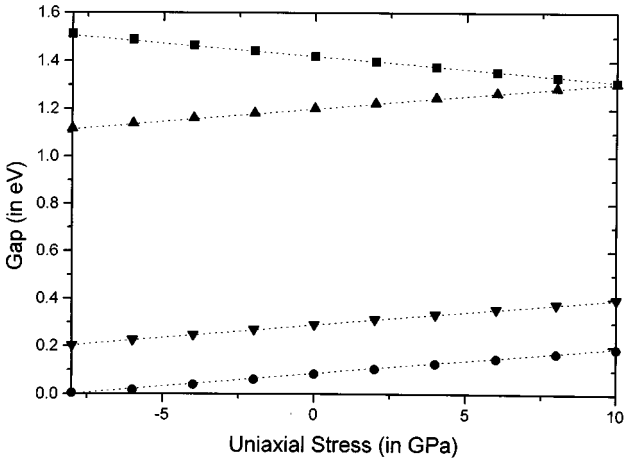

FIG. 3. Band gap as a function of stress: circle, square, and up triangle correspond, respectively to a small band gap (9,0) and moderate band gaps (8,0) and (10,0). For these three tubules, $q=3$. The down triangle corresponds to a (40,0) tubule (diameter of 3.1 nm).

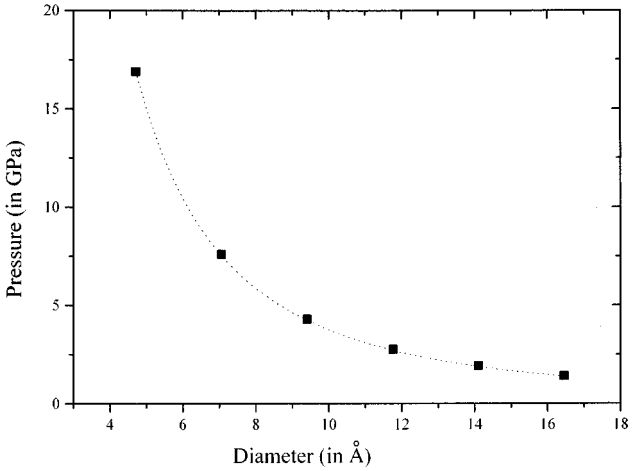

FIG. 4. Variation of semiconductor to metal transition pressure with diameter for $(3q,0)$ tubules.

forms: $(3q,0)$, $(3q+1,0)$, or $(3q-1,0)$, where q is an integer. The electronic band gap is always obtained by setting $m=q$ in formula (4.5). For example, if the zigzag tubule satisfies $(3q,0)$ we obtain the following expression of the gap E_g:

$$E_g(\sigma)=2|t_3-t_{12}-V_{12}|. \tag{4.6}$$

Given that the values of S_{11} and S_{12} are of the order of 10^{-12} Pa^{-1}, the products σS_{11} and σS_{12} are small compared to unity for strains less than 10 GPa. Consequently, formula (4.6) can be developed near $\sigma S_{11}=0$ and we obtain, neglecting the small curvature term,

$$E_g(\sigma)\simeq 3t_0(S_{11}-S_{12})\sigma, \tag{4.7}$$

where $t_0=3.2$ eV (Ref. 13) is the two-center integral between π orbitals of nearest neighbors in the graphene.

Using the values of S_{11} and S_{12} given above, expression (4.7) shows that the gap sensitivity with stress is equal to 10.7 meV/GPa for uniaxial stress less than 10 GPa. This value is comparable to that found for various diamond structures[24] or semiconductor such as GaAs.[23]

As indicated in Fig. 3, the variation of $E_g=E_g(\sigma)$ in the case of $(3q-1,0)$ and $(3q+1,0)$ nanotubes remains linear with approximatively the same value for $|dE_{\mathrm{gap}}/d\sigma|$. Figure 3 allows proposing a different classification for the zigzag tubules. In the case of $(3q+1,0)$, the gap increases under traction, whereas in the case $(3q-1,0)$ it decreases. These different kinds of behavior can be understood in the 2D representation by examining the effects of stress on the allowed lines in the Brillouin zones. In the $(3q+1,0)$ case, the nearest corner allowed line moves away from the K point, whereas for the $(3q-1,0)$ case it becomes closer.

Furthermore, we observe on Fig. 3 that compression should lead to a semiconductor to metal transition in the case of $(3q,0)$ and $(3q+1,0)$ and the same kind of transition is obtained with traction in the case of $(3q-1,0)$ tubules, at a diameter dependent stress $\sigma_t(d)$. In their study of instabilities beyond linear response theory Yakobson *et al.*[25] showed that a tubule modeled by a Tersoff-Brenner potential,[26,27] shows four singularities at high strains ϵ when subjected to uniaxial compression. If ϵ is less than 0.05 there is no shape change. In our case, this value corresponds to an axial stress inferior to 51 GPa. It should be noted that prior to this work of Yacobson *et al.*,[25] Robertson *et al.*[28] presented one of the first studies on stress effects: the variation of strain energy with tubule diameter, chirality, and uniform tensile strain.

We observe from Fig. 3 that only the $(3q,0)$ tubules might present such an experimentally observable transition as shown on Fig. 4. Figure 4 represents the stress at which the semiconductor to metal transition occurs for $(3q,0)$ zigzag tubules. Thus, knowledge of a given tubule's diameter would allow predicting the stress necessary to create a semiconducting tubule of a given gap or the stress required to obtain metallic behavior.

V. CONCLUSION

In summary, we have shown that a uniaxial stress applied parallel to the axis of carbon nanotubes can significantly modify the band gap and induce a semiconductor-metal transition. For the zigzag tubules $(n,0)$ the behavior is strongly dependent on whether $n=3q$, $3q-1$, or $3q+1$. As for the DOS, an analytic expression has been put forth using 1D Green's-function theory. From an experimental viewpoint, state of the art nanotechnology has recently permitted measuring the galvanomagnetic properties of a single bundle[29,30] and a single nanotube.[10] Furthermore, recent studies have allowed determination of the elastic properties of microstructures such as DNA chains.[31] Adaptation of such technologies may therefore open the future to experimental works under the effects of stress.

[1] S. Iijima, Nature **354**, 56 (1991).
[2] J. W. Mintmire, B. I. Dunlap, and C. T. White, Phys. Rev. Lett. **68**, 631 (1992).
[3] N. Hamada, S. Sawada, and A. Oshiyama, Phys. Rev. Lett. **68**, 1579 (1992).
[4] R. Saito, M. Fujita, G. Dresselhaus, and M. S. Dresselhauss, Phys. Rev. B **46**, 1804 (1992).
[5] K. Tanaka, K. Okahara, M. Okada, and T. Yamabe, Chem. Phys. Lett. **191**, 469 (1992).
[6] J. W. Mintmire and C. T. White, Carbon **33**, 893 (1995).
[7] M. S. Dresselhauss, Nature **358,** 195 (1992).
[8] G. Overney, W. Zhong, and D. Tomanek, Z. Phys. D **27**, 93 (1993).
[9] J. Tersoff and R.S. Ruoff, Phys. Rev. Lett. **73**, 676 (1994).
[10] H. Dai, E.W. Wong, and C.M. Lieber, Science **272**, 523 (1996).
[11] M. S. Dresselhaus, G. Dresselhaus, and R. Saito, Carbon **33**, 883 (1995).
[12] R. Heyd, A. Charlier, E. McRae, J.F. Marêché, and M.F. Charlier, in *The 22nd Biennal Conference on Carbon, San Diego, 1995* (University of San Diego, San Diego, 1995), pp. 346 and 347.
[13] J.C. Charlier, J.P. Micheneaud, X. Gonze, and J.P. Vigneron, Phys. Rev. B **44**, 13 237 (1991).
[14] E.N. Economou, in *Green's Functions in Quantum Physics*, edited by E. H. Lieb, Springer Series in Solid-State Sciences Vol. 7 (Springer-Verlag, Berlin, 1990).
[15] B.A. McKinnon and T.C. Choy, Aust. J. Phys. **46**, 601 (1993).
[16] R. Saito, G. Dresselhaus, and M. S. Dresselhauss, J. Appl. Phys. **73**, 494 (1993); M. S. Dresselhaus, G. Dresselhaus, and R. Saito, Solid State Commun. **84**, 201 (1992).
[17] C.H. Olk and J.P. Heremans, J. Mater. Res. **9**, 259 (1994).
[18] Q.M. Ma, K.L. Wang, and J.N. Schulman, Phys. Rev. B **47**, 1936 (1993).
[19] J.F. Nye, *Physical Properties of Crystal* (Clarendon, Oxford, 1985).
[20] B.T. Kelly, *Physics of Graphite* (Applied Science, London, 1981).
[21] W.A. Harrison, *Electronic Structure and Properties of Solids* (Freeman, San Francisco, 1980).
[22] C. Priester, G. Allan, and M. Lanno, Phys. Rev. B **37**, 8519 (1988).
[23] S.Y. Ren, J.D. Dow, and D.J. Wolford, Phys. Rev. B **25**, 7661 (1982).
[24] S. Fahy and S.G. Louie, Phys. Rev. B **36**, 3373 (1987).
[25] B.I. Yakobson, C.J. Babec, and J. Bernholc, Phys. Rev. Lett. **76**, 2511 (1996).
[26] J. Tersoff, Phys. Rev. B **37**, 6991 (1988).
[27] D.W. Brenner, Phys. Rev. B **42**, 9458 (1990).
[28] D.H. Robertson, D.W. Brenner, and J.W. Mintmire, Phys. Rev. B **45**, 12 592 (1992).
[29] J.P. Issi, L. Langer, J. Heremans, and C.H. Olk, Carbon **33**, 941 (1995).
[30] L. Langer, V. Bayot, E. Grivei, and J.P. Issi, Phys. Rev. Lett. **76**, 479 (1996).
[31] J.F. Marko and E.D. Siggia, Science **265**, 1599 (1994); D. Bensimon, A.J. Simon, V. Croquette, and A. Bensimon, Phys. Rev. Lett. **74**, 4754 (1995).